

Original Research

# Analysis of Dengue Transmission Dynamic Model by Stability and Hopf Bifurcation with Two-Time Delays

Prakash Raj Murugadoss<sup>1</sup>, Venkatesh Ambalarajan<sup>1</sup>, Vinoth Sivakumar<sup>2</sup>,  
Prasanth Bharathi Dhandapani<sup>3,\*</sup>, Dumitru Baleanu<sup>4,5,6,\*</sup><sup>1</sup>Department of Mathematics, A.V.V.M. Sri Pushpam College (Affiliated to Bharathidasan University, Tiruchirappalli), Poondi, 613 503 Thanjavur, Tamil Nadu, India<sup>2</sup>Department of Mathematics, V.S.B. Engineering College, 639111 Karur, Tamil Nadu, India<sup>3</sup>Department of Mathematics, Sri Eshwar College of Engineering, 641202 Coimbatore, Tamil Nadu, India<sup>4</sup>Department of Mathematics, Cankara University, 06530 Ankara, Turkey<sup>5</sup>Institute of Space Sciences, Laboratory of Theoretical Physics, R 76900, Magurele-Bucharest, Romania<sup>6</sup>Department of Natural Sciences, School of Arts and Sciences, Lebanese American University, 11022801 Beirut, Lebanon\*Correspondence: [d.prasanthbharathi@gmail.com](mailto:d.prasanthbharathi@gmail.com) (Prasanth Bharathi Dhandapani); [dumitru.baleanu@gmail.com](mailto:dumitru.baleanu@gmail.com) (Dumitru Baleanu)

Academic Editors: Yeliz Karaca, Dumitru Baleanu, Yu-Dong Zhang, Majaz Moonis, Osvaldo Gervasi and Khan Muhammad

Submitted: 22 March 2023 Revised: 26 April 2023 Accepted: 5 May 2023 Published: 25 June 2023

## Abstract

**Background:** Mathematical models reflecting the epidemiological dynamics of dengue infection have been discovered dating back to 1970. The four serotypes (DENV-1 to DENV-4) that cause dengue fever are antigenically related but different viruses that are transmitted by mosquitoes. It is a significant global public health issue since 2.5 billion individuals are at risk of contracting the virus. **Methods:** The purpose of this study is to carefully examine the transmission of dengue with a time delay. A dengue transmission dynamic model with two delays, the standard incidence, loss of immunity, recovery from infectiousness, and partial protection of the human population was developed. **Results:** Both endemic equilibrium and illness-free equilibrium were examined in terms of the stability theory of delay differential equations. As long as the basic reproduction number ( $R_0$ ) is less than unity, the illness-free equilibrium is locally asymptotically stable; however, when  $R_0$  exceeds unity, the equilibrium becomes unstable. The existence of Hopf bifurcation with delay as a bifurcation parameter and the conditions for endemic equilibrium stability were examined. To validate the theoretical results, numerical simulations were done. **Conclusions:** The length of the time delay in the dengue transmission epidemic model has no effect on the stability of the illness-free equilibrium. Regardless, Hopf bifurcation may occur depending on how much the delay impacts the stability of the underlying equilibrium. This mathematical modelling is effective for providing qualitative evaluations for the recovery of a huge population of afflicted community members with a time delay.

**Keywords:** dengue transmission; reproduction number; Hopf bifurcation; time delay; stability; medical implications

## 1. Introduction

Dengue fever is a critical feverish illness caused by mosquito-borne dengue fever viruses (DENV) [1], which are Flaviviridae flaviviruses. When an infected *Aedes aegypti* mosquito infects a person, many viruses are transmitted. The transmission of the dengue virus is mostly carried out by humans. A virus-infected mosquito feeds on the blood of a virus-infected person. The virus spreads to tissues such as the duct gland from the mosquito's gut in 8–10 days. The virus appears to have no negative influence on the mosquito. When a DENV-carrying mosquito bites a human, both the virus and the mosquito's secretions are injected into the skin. As it circulates throughout the body, it clings to and enters white blood cells, multiplying in them. White blood cells produce a number of signal proteins in response, including interferon, which can lead to symptoms including fever, flu-like symptoms, and excruciating pains.

A variety of organs, including the liver and bone marrow, are regularly damaged by serious infections. They also

increase the body's production of viruses and frequently cause fluid to leak from the circulation into internal organ cavities via the membranes of tiny blood vessels. As a consequence, blood pressure drops to a level where many organs are unable to get enough blood due to decreased blood flow in the blood vessels. The other major effect of dengue fever is bleeding, which was made more likely by bone marrow diseases that decreased the quantity of platelets needed for effective blood coagulation [2].

We provide an associative model that supports the susceptible-infective-recovery-susceptible (SIRS) in the human population and the susceptible-infective (SI) in the vector (mosquito) population while avoiding delays in a trial to examine the dynamics of infection across considerable time periods when susceptible people are born and immunity is lost. Because of vector dynamics, the vector population is typically regarded as being in equilibrium with the human population [3,4]. The analysis of the delay differential equation in the epidemic model was studied in [5–7].



The transmission process between humans and mosquitoes takes a long time because of the different parasites' incubation times [2,8]. The dynamics of dengue virus transmission with a delayed SIVA model are studied in [9]. Sefidgar *et al.* [10] discussed the nonlinear system of fractional differential equations that appear in a model of HIV infection of CD4+T cells and proposed the LAM for solving the system. The results showed the effectiveness and efficiency of the method. Wei *et al.* [11] developed a system for a vector-borne disease with a direct method of transmission, but they also showed how the addition of a latency inside the host-to-vector transmitter term will make the system unstable and cause periodic solutions through Hopf bifurcation.

Omame *et al.* [12] formulated a mathematical model for the co-infection, COVID-19 and dengue transmission dynamics with optimal control and cost-effectiveness analysis. The results showed that the strategy for implementing control against incident dengue infection is the most cost-effective in controlling dengue and COVID-19 co-infection. Omame *et al.* [13] design a non-integer ordered model for SARS-CoV-2, dengue, and HIV co-dynamics to assess the impact of SARS-CoV-2 infection on the dynamics of dengue and HIV through fractional derivatives. They showed, using numerical simulations, that keeping the spread of SARS-CoV-2 low would have a significant impact on reducing the co-infections of SARS-CoV-2 and dengue or SARS-CoV-2 and HIV. Based on SIRS-SI in the human and vector populations, Wan and Cui [14] presented a model that utilized two latencies for communication between humans and vector populations with the standard incidence rate, loss of immunity, and rate of recovery from infectiousness. To explore the possibility of equilibrium stability and dynamic behavior, Xu and Zhou [15] projected the dynamics of delayed vector-borne transmission with reinfection. An epidemic model with vaccination and numerous time delays is taken into account in [16] along with the stability and Hopf bifurcation analysis. Baleanu and Babak [17] studied a terminal value problem for nonlinear systems of generalized fractional differential equations and formulated a classical operator and a related weighted space with a generalized fractional operator. The results showed the effects of various choices of weight function on modeling with a TVP. Nowadays, many authors do their research on epidemic models [18–20] with various strategies. To take into consideration the amount of time required for a viral infection to spread to host and vector populations, Yanxia *et al.* [21] design an associated upgraded vector-borne epidemic model with two latency periods and reinfection. We created a new model using the information in this article and included three new parameters, including loss of immunity, recovery from infectiousness, and partial protection of the human population.

In this paper, the basic reproduction number for the developed model was determined, and the existence of equilibrium was also examined. The aim of the paper is to

explore the stability and Hopf bifurcation of a dynamic model of dengue transmission that incorporates two delays. The numerical simulations were described, and the main conceptual outcomes were exhibited. Fig. 1 provides a schematic overview of this model.

## 2. Model Formulation

The model considers a uniform mix of human and mosquito populations, ensuring that every mosquito bite provides the same possibility of spreading the virus (or transmitting the virus from an infected human). Because mosquitoes cannot recover from infection, their infection period ends when they die, owing to their incredibly short lifespan. As a result, the mosquito population has a relatively low immunity class, and mortality rates are comparable across all categories.

$H_N(t)$  represents the whole human population at time  $t$ , which is divided into three compartments: susceptible humans  $S_H(t)$ , infectious humans  $I_H(t)$ , and recovered humans  $R_H(t)$ . So, the entire human population is  $H_N(t) = S_H(t) + I_H(t) + R_H(t)$ .

Similarly,  $V_N(t)$  represents the whole mosquito population at time  $t$ , which is divided into two compartments: susceptible vector  $S_V(t)$  and infectious vector  $I_V(t)$ . So, the entire vector population is  $V_N(t) = S_V(t) + I_V(t)$ .

Assumptions of the model:

(a) The human and vector total population sizes are considered to be constant. It is expected that new humans will enter the human population at any time at  $\Omega_H$  rate through birth or immigration, and those susceptible mosquitoes will be recruited at a constant rate  $\Omega_V$ .

(b) Depending on the sickness, people shift from one class to another as their health improves. This infusion is not contagious since there is no vertical transmission or immigration of affected persons. When the *Aedes aegypti* mosquito bites the host, all people get infected, and dengue development begins.

(c) Natural death occurs at a rate of  $d_h$  and  $d_v$  [21] (according to their limited life span) for all humans and mosquitoes respectively, regardless of condition.

(d) Individuals who have recovered in the human population acquire partial immunity ( $\sigma$ ) or loss of immunity ( $\rho$ ) [21].

(e) Illness mortality rates for humans and mosquitoes are  $\mu_h$  and  $\mu_v$ , respectively.

(f) The term  $e^{-d_h\tau_1}$  and  $e^{-d_v\tau_2}$  is the human and mosquito survival rate [22].

(g) Mosquitoes do not die or become infected by infection.

The system of non-linear differential equations for the dengue model is

$$\begin{aligned} \frac{dS_H}{dt} = & \Omega_H - \alpha\beta_h S_H(t - \tau_1) I_V(t - \tau_1) e^{-d_h\tau_1} \\ & - d_h S_H + \theta I_H + \rho R_H \end{aligned} \quad (1)$$

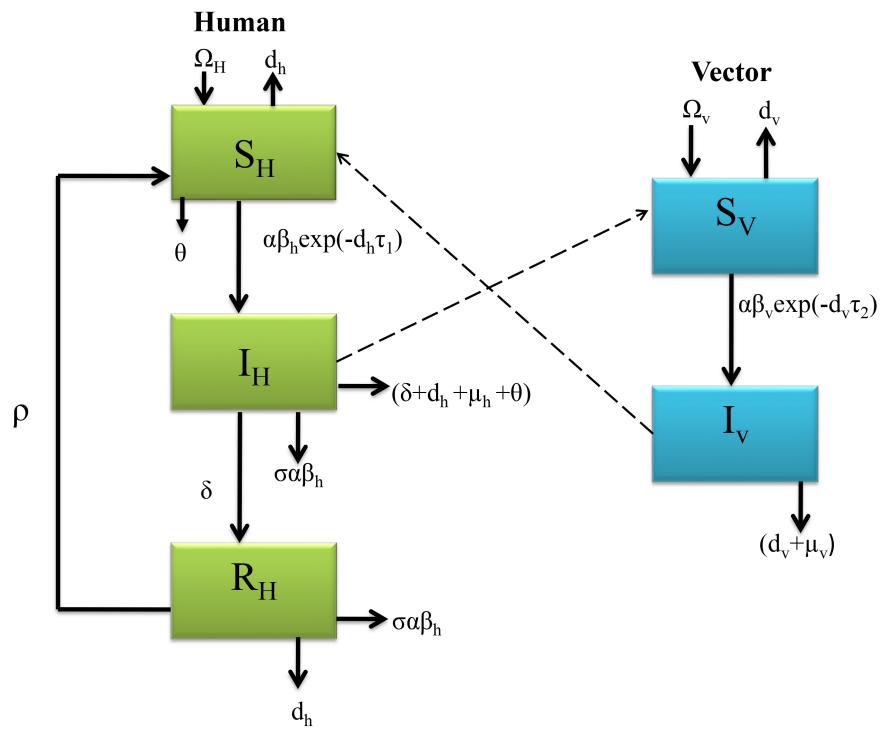


Fig. 1. Schematic diagram of dengue transmission.

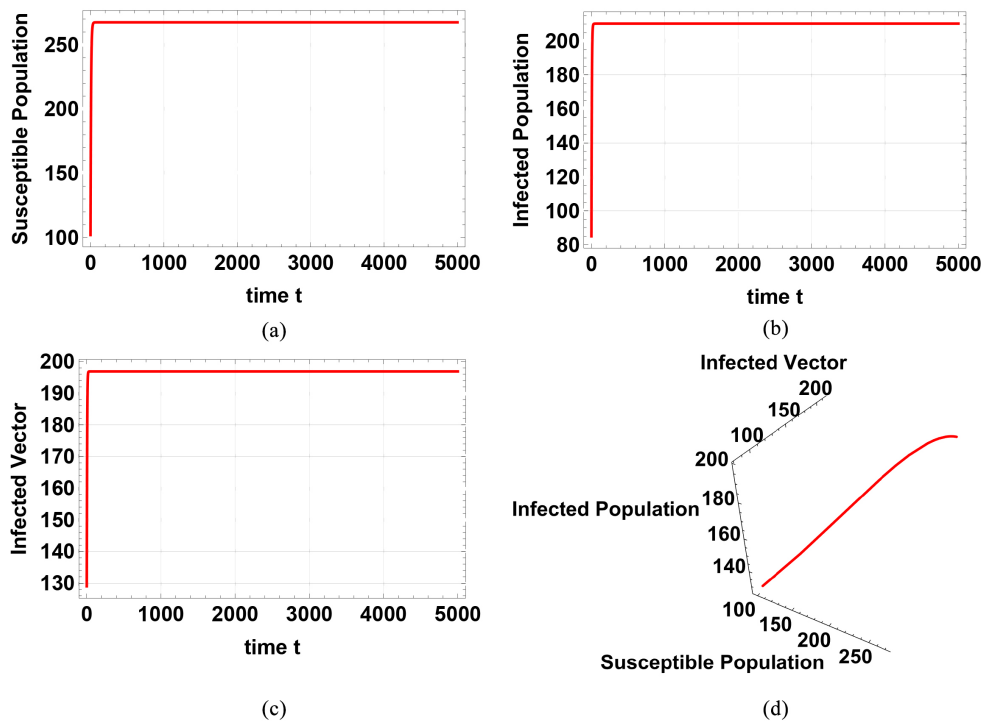
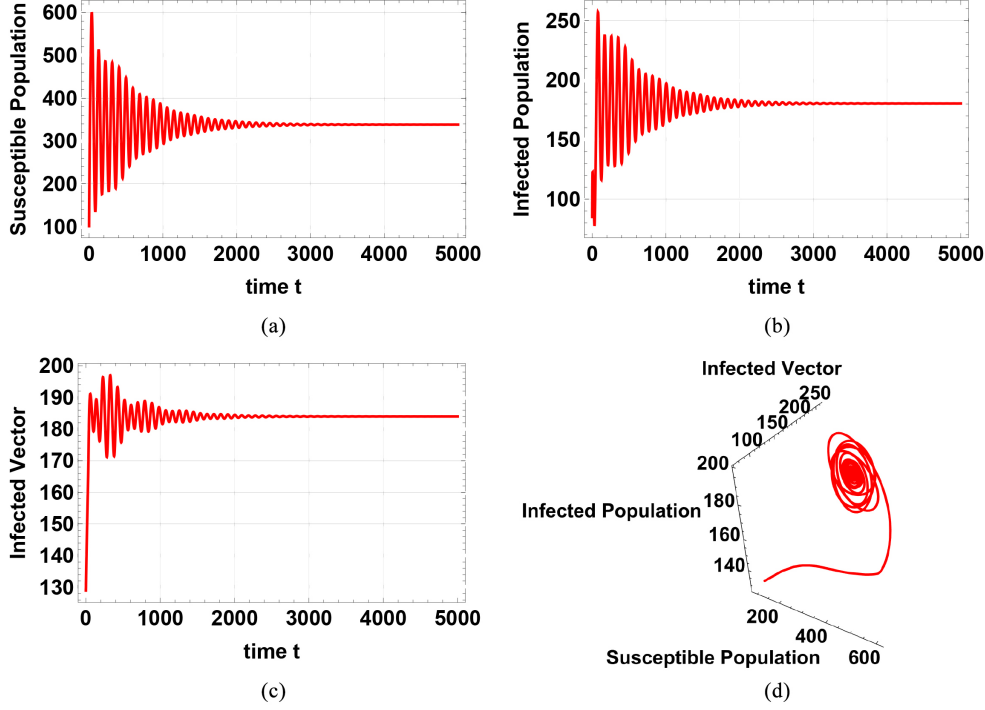


Fig. 2. When  $\tau_1 = \tau_2 = 0$ ,  $E^*$  of the system Eqn. 7 is locally asymptotically stable. (a) The force of the susceptible population converges to the positive equilibrium value  $S_H^* = 267.781$ . (b) The force of the infected population converges to the positive equilibrium value  $I_H^* = 210.142$ . (c) The force of the infected vector converges to the positive equilibrium value  $I_V^* = 196.792$ . (d) Phase diagram of  $E^*$ .



**Fig. 3.** When  $\tau_1 > 0$  and  $\tau_2 > 0$ ,  $E^*$  of the system Eqn. 7 is locally asymptotically stable. (a) The force of the susceptible population converges to the positive equilibrium value  $S_H^* = 339.886$ . (b) The force of the infected population converges to the positive equilibrium value  $I_H^* = 180.022$ . (c) The force of the infected vector converges to the positive equilibrium value  $I_V^* = 183.872$ . (d) Phase diagram of  $E^*$ .

$$\frac{dI_H}{dt} = \alpha\beta_h S_H(t - \tau_1) I_V(t - \tau_1) e^{-d_h \tau_1} + \sigma\alpha\beta_h R_H I_V - (\delta + d_h + \mu_h + \theta) I_H \quad (2)$$

$$\frac{dR_H}{dt} = \delta I_H - \sigma\alpha\beta_h R_H I_V - (d_h + \rho) R_H \quad (3)$$

$$\frac{dS_V}{dt} = \Omega_V - \alpha\beta_V S_V(t - \tau_2) I_H(t - \tau_2) e^{-d_v \tau_2} - d_v S_V \quad (4)$$

$$\frac{dI_V}{dt} = \alpha\beta_V S_V(t - \tau_2) I_H(t - \tau_2) e^{-d_v \tau_2} - (d_v + \mu_v) I_V \quad (5)$$

with the following initial conditions:

$$\begin{aligned} S_H(\psi) &= S_{0H}(\psi), I_H(\psi) = I_{0H}(\psi), R_H(\psi) = R_{0H}(\psi) \\ S_V(\psi) &= S_{0V}(\psi), I_V(\psi) = I_{0V}(\psi) \\ H_N(\psi) &= H_{0N}(\psi), V_N(\psi) = V_{0N}(\psi) \\ \psi &\in [-\tau, 0], \tau = \max\{\tau_1, \tau_2\} \end{aligned} \quad (6)$$

The systems Eqn. 1 to Eqn. 5 is reformulated as

$$\begin{aligned} \frac{dS_H}{dt} &= \Omega_H - \alpha\beta_h S_H(t - \tau_1) I_V(t - \tau_1) e^{-d_h \tau_1} - d_h S_H \\ &\quad + \theta I_H + \rho \left( \frac{\Omega_H}{d_h} - S_H - I_H \right) \\ \frac{dI_H}{dt} &= \alpha\beta_h S_H(t - \tau_1) I_V(t - \tau_1) e^{-d_h \tau_1} + \\ &\quad \sigma\alpha\beta_h \left( \frac{\Omega_H}{d_h} - S_H - I_H \right) I_V - (\delta + d_h + \mu_h + \theta) I_H \\ \frac{dI_V}{dt} &= \alpha\beta_V \left( \frac{\Omega_V}{d_v} - I_V(t - \tau_2) \right) I_H(t - \tau_2) e^{-d_v \tau_2} \\ &\quad - (d_v + \mu_v) I_V \end{aligned} \quad (7)$$

The parameters of the above system Eqn. 7 is described in Table 1.

### 3. Model Analysis

#### 3.1 Positivity and Boundedness Solution of Dengue Transmission Dynamic Model

The solution of the system Eqn. 7 is usually positive for positive initial values of the data at all times  $t \geq 0$ . Especially, the feasible region is  $C = \{ (S_H, I_H, I_V) \in \mathbb{R}_+^3 \mid 0 \leq S_H + I_H \leq \frac{\Omega_H}{d_h}, 0 \leq I_V \leq \frac{\Omega_V}{d_v}, S_H \geq 0, I_H \geq 0, I_V \geq 0 \}$ .

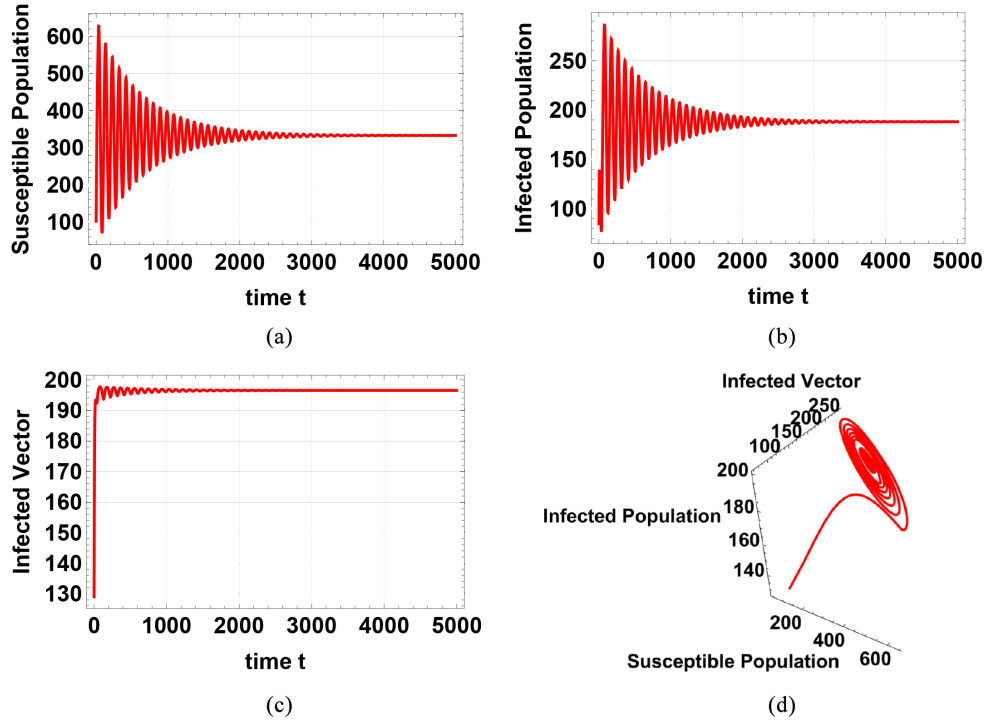


**Fig. 4.** When  $\tau_1 = 32.8 > \tau_1^*$  and  $\tau_2 = 0$ ,  $E^*$  of the system Eqn. 7 is locally asymptotically stable. (a) The force of the susceptible population converges to the positive equilibrium value  $S_H^* = 333.986$ . (b) The force of the infected population converges to the positive equilibrium value  $I_H^* = 188.115$ . (c) The force of the infected vector converges to the positive equilibrium value  $I_V^* = 196.753$ . (d) Phase diagram of  $E^*$ .

**Table 1. Parameters of the model.**

Parameter	Description
$\Omega_H$	the rate of human recruitment population
$\Omega_V$	the rate of mosquito recruitment population
$\beta_h$	infection rate from mosquitoes in humans
$\beta_v$	infection rate from humans in mosquitoes
$d_h$	the natural death rate of the human population
$d_v$	the natural death rate of the vector population
$\mu_h$	the illness-induced death rate of the human population
$\mu_v$	the illness-induced death rate of the mosquito population
$\alpha$	the biting rate of Aedes aegypti mosquitoes per day
$\theta$	the individual rate of recovery for a class susceptible to infection
$\delta$	recovery rate of the infected human population
$\sigma$	partial immunity for people who have recovered from the initial illness
$\rho$	individual rate of immune loss in the human population
$\tau_1$	extrinsic incubation period of time delay from susceptible to infectious class in populations of humans
$\tau_2$	intrinsic incubation period of time delay from susceptible to infectious class in populations of mosquitoes

### Theorem 1

The feasible region  $C = \{ (S_H, I_H, I_V) \in R_+^3 \mid 0 \leq S_H + I_H \leq \frac{\Omega_H}{d_h}, 0 \leq I_V \leq \frac{\Omega_V}{d_v}, S_H \geq 0, I_H \geq 0, I_V \geq 0 \}$  is positively-invariant for the system Eqn. 7.

### Proof

According to [23,24], it is easy to show that the solution of the Eqns. 1 to 5 with the initial conditions Eqn. 6 is

distinct and nonnegative for all  $t \geq 0$ , based on the fundamental theory of differential equations.

From Eqns. 1 to 3, the rate of change of whole human population is given by

$$H'_N(t) = \Omega_H - d_h H_N - \mu_h I_H \quad (8)$$

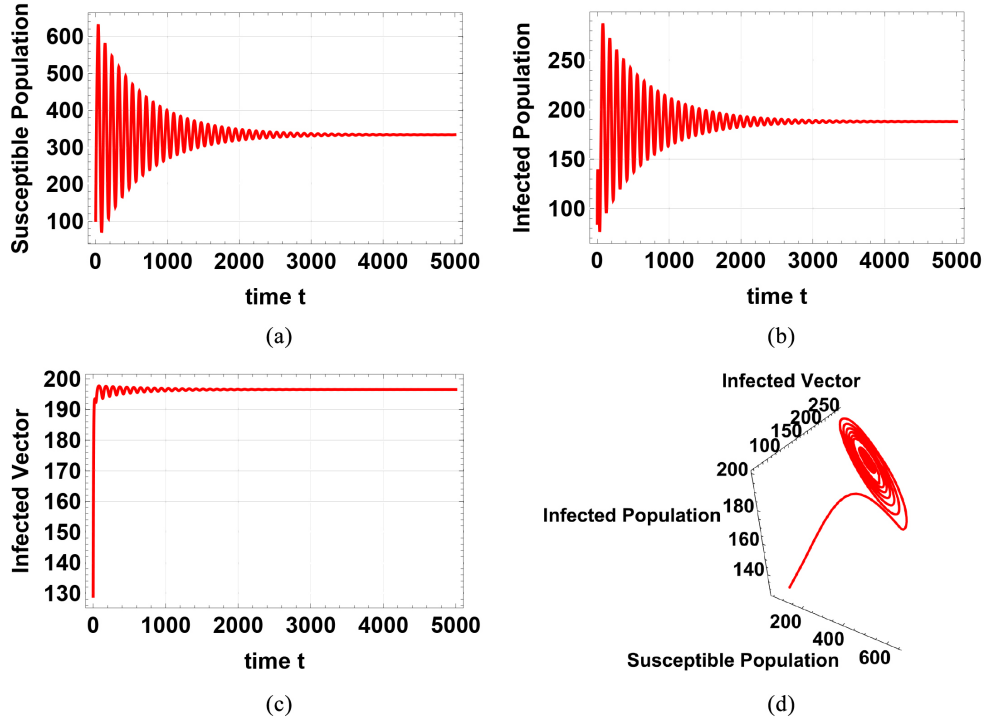


**Fig. 5.**  $E^*$  of the system Eqn. 7 is unstable and a Hopf bifurcation occurring in  $\tau_1 = 33 > \tau_1^*$  and  $\tau_2 = 0$ . (a) The force of the susceptible population diverges to the positive equilibrium. (b) The force of the infected population diverges to the positive equilibrium. (c) The force of the infected vector diverges to the positive equilibrium. (d) Phase diagram of  $E^*$ .

Without loss of generality, this equation can be expressed as an inequality as

$$H'_N(t) \leq \Omega_H - d_h H_N$$

$$H_N(t) \leq \frac{\Omega_H}{d_h} + \left[ H_{0N} - \left( \frac{\Omega_H}{d_h} \right) \right] \exp(-d_h t).$$

Then,  $\lim_{t \rightarrow \infty} H_N(t) \leq \frac{\Omega_H}{d_h}$ .

Therefore,  $H_N(t)$  is bounded.

From Eqns. 4 to 5, the rate of change of whole mosquito population is given by

$$V'_N(t) = \Omega_V - d_v V_N - \mu_v I_V \quad (9)$$

Without loss of generality, this equation can be expressed as an inequality as

$$V'_N(t) \leq \Omega_V - d_v V_N$$

$$V_N(t) \leq \frac{\Omega_V}{d_v} + \left[ V_{0N} - \left( \frac{\Omega_V}{d_v} \right) \right] \exp(-d_v t).$$

Then,  $\lim_{t \rightarrow \infty} V_N(t) \leq \frac{\Omega_V}{d_v}$ .

Therefore,  $V_N(t)$  is bounded.

By limits theorem,  $0 \leq S_H + I_H \leq H_N(t) < \left( \frac{\Omega_H}{d_h} \right) + \epsilon$  holds for all  $t \rightarrow \infty$ .

Then for any,  $\epsilon > 0$ ,  $0 \leq S_H + I_H \leq \frac{\Omega_H}{d_h}$ .

Similarly,  $0 \leq I_V \leq \frac{\Omega_V}{d_v}$ .

Thus, the region  $C = \{ (S_H, I_H, I_V) \in R_+^3 \mid 0 \leq S_H + I_H \leq \frac{\Omega_H}{d_h}, 0 \leq I_V \leq \frac{\Omega_V}{d_v}, S_H \geq 0, I_H \geq 0, I_V \geq 0 \}$  is positively-invariant for the system (Eqn. 7).

### 3.2 Basic Reproduction Number of the Model

The illness-free equilibrium,  $E^0 = \{S_H^0, I_H^0, I_V^0\}$  is the model's steady state in the lack of infection or illness. All the components of  $E^0$  are determined from the first three equations of system Eqn. 7 by putting the RHS equal to zero and assuming that  $I_H^0 = 0$  and  $I_V^0 = 0$ , where  $I_H^0$  and  $I_V^0$  refer to the equilibrium points.

Thus,

$$E^0 = \left\{ \frac{\Omega_H}{d_h + \rho}, 0, 0 \right\} \quad (10)$$

The next generation matrix technique, as designated by Diekmann *et al.* [25], was used to determine the basic reproduction number  $R_0$ .

From system Eqn. 7, the illness states A and the transfer states B are given by

$$A = \begin{bmatrix} \alpha \beta_h S_H I_V e^{-d_h \tau_1} \\ \alpha \beta_v S_V I_H e^{-d_v \tau_2} \end{bmatrix} \text{ and } B = \begin{bmatrix} (\delta + d_h + \mu_h + \theta) I_H \\ (d_v + \mu_v) I_V \end{bmatrix} \text{ respectively.}$$

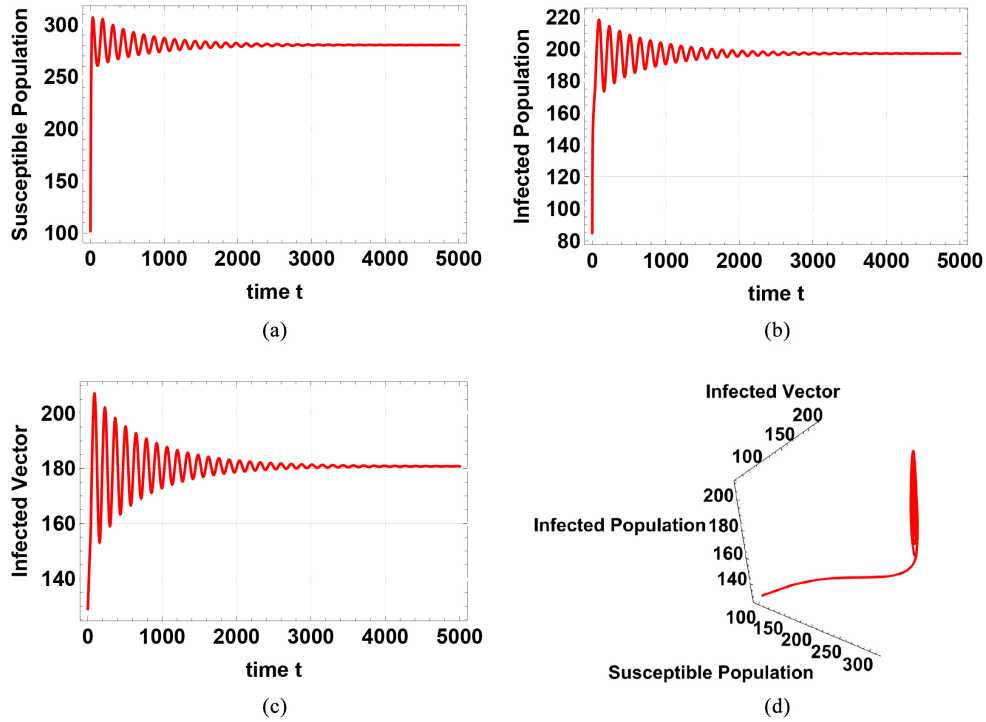


**Fig. 6.** When  $\tau_1 = 0$  and  $\tau_2 = 36 < \tau_2^*$ , the system Eqn. 7 is unstable and a Hopf bifurcation occurring. (a) The force of the susceptible population diverges to the positive equilibrium. (b) The force of the infected population diverges to the positive equilibrium. (c) The force of the infected vector diverges to the positive equilibrium. (d) Phase diagram of  $E^*$ .

Using Jacobian matrix, the partial derivatives of A and B with respect to  $I_H$  and  $I_V$  at the illness-free equilibrium Eqn. 10, are given by

$$F = \begin{bmatrix} 0 & \alpha\beta_h \frac{\Omega_H}{d_h + \rho} e^{-d_h \tau_1} \\ \alpha\beta_v \frac{\Omega_V}{d_v} e^{-d_v \tau_2} & 0 \end{bmatrix} \text{ and } V = \begin{bmatrix} (\delta + d_h + \mu_h + \theta) & 0 \\ 0 & (d_v + \mu_v) \end{bmatrix}$$

Now the next generation matrix  $FV^{-1}$  can be calculated as

$$FV^{-1} = \begin{bmatrix} 0 & \frac{\alpha\beta_h \Omega_H e^{-d_h \tau_1}}{(d_h + \rho)(d_v + \mu_v)} \\ \frac{\alpha\beta_v \Omega_V e^{-d_v \tau_2}}{d_v (\delta + d_h + \mu_h + \theta)} & 0 \end{bmatrix} \quad (11)$$

The eigenvalues of Eqn. 11 are used to derive the basic reproduction number, which is

$$R_0 = \frac{\alpha^2 \beta_h \beta_v \Omega_H \Omega_V e^{-d_h \tau_1} e^{-d_v \tau_2}}{(d_h + \rho) d_v (d_v + \mu_v) (\delta + d_h + \mu_h + \theta)} \quad (12)$$

### 3.3 Endemic Equilibrium Existence of the Model

The endemic equilibrium  $E^*$ , is the model's stable state in which the illness continues. All the components of  $E^*$  are obtained from the system Eqn. 7 by framing the right-hand side equal to zero.

Thus,

$$E^* = \{S_H^*, I_H^*, I_V^*\} \quad (13)$$

where

$$S_H^* = \frac{\left(\left(\frac{\Omega_H}{d_h}\right)\rho + \Omega_H + (\theta - \rho)I_H^*\right)(\alpha\beta_v I_H^* e^{-d_v \tau_2} + (d_v + \mu_v))}{(d_h + \rho)(\alpha\beta_v I_H^* e^{-d_v \tau_2} + (d_v + \mu_v)) + \left(\frac{\Omega_V}{d_v}\right)\alpha^2 \beta_h \beta_v I_H^* e^{-d_h \tau_1} e^{-d_v \tau_2}}$$

$$I_V^* = \frac{\left(\frac{\Omega_V}{d_v}\right)\alpha\beta_v I_H^* e^{-d_v \tau_2}}{\alpha\beta_v I_H^* e^{-d_v \tau_2} + (d_v + \mu_v)}$$

$I_H^*$  is the positive root of the quadratic equation shown below

$$X_1 I_H^{*2} + X_2 I_H^* + X_3 = 0 \quad (14)$$

where

$$X_1 = \alpha\beta_v^2 e^{-2d_v \tau_2} \left[ \alpha\beta_h \left(\frac{\Omega_V}{d_v}\right) e^{-d_h \tau_1} - d_h \right] (\delta + \rho + d_h + \mu_h) + \sigma \alpha^2 \beta_h \beta_v \left(\frac{\Omega_V}{d_v}\right) e^{-2d_v \tau_2}$$

$$[ \alpha\beta_h \beta_v \left(\frac{\Omega_V}{d_v}\right) e^{-d_h \tau_1} - (\theta + d_h) ]$$

$$- \alpha\beta_v^2 e^{-2d_v \tau_2} [ \rho(\delta + \theta) + \mu_h(\rho + d_h) ]$$

$$X_2 = \alpha^2 \beta_h \beta_v^2 \left(\frac{\Omega_V}{d_v}\right) e^{-2d_v \tau_2} \left[ \rho \left(\frac{\Omega_H}{d_h}\right) e^{-d_h \tau_1} \right.$$

$$\left. \sigma \left(\frac{\Omega_H}{d_h}\right) d_h - \Omega_H \right] + e^{-d_h \tau_1} \left[ \sigma \alpha \beta_h \left(\frac{\Omega_H}{d_h}\right) \left(\frac{\Omega_V}{d_v}\right) - \Omega_H \right]$$

$$- \alpha\beta_v (d_v + \mu_v) (\delta + \theta + \rho + d_h) [ 2d_h + \alpha\beta_h \left(\frac{\Omega_V}{d_v}\right) e^{-d_h \tau_1} ]$$

$$e^{-d_v \tau_2} - \alpha\beta_v (d_v + \mu_v) e^{-d_v \tau_2} [ 2\mu_h(\rho + d_h) + \sigma \alpha \beta_h (\theta +$$

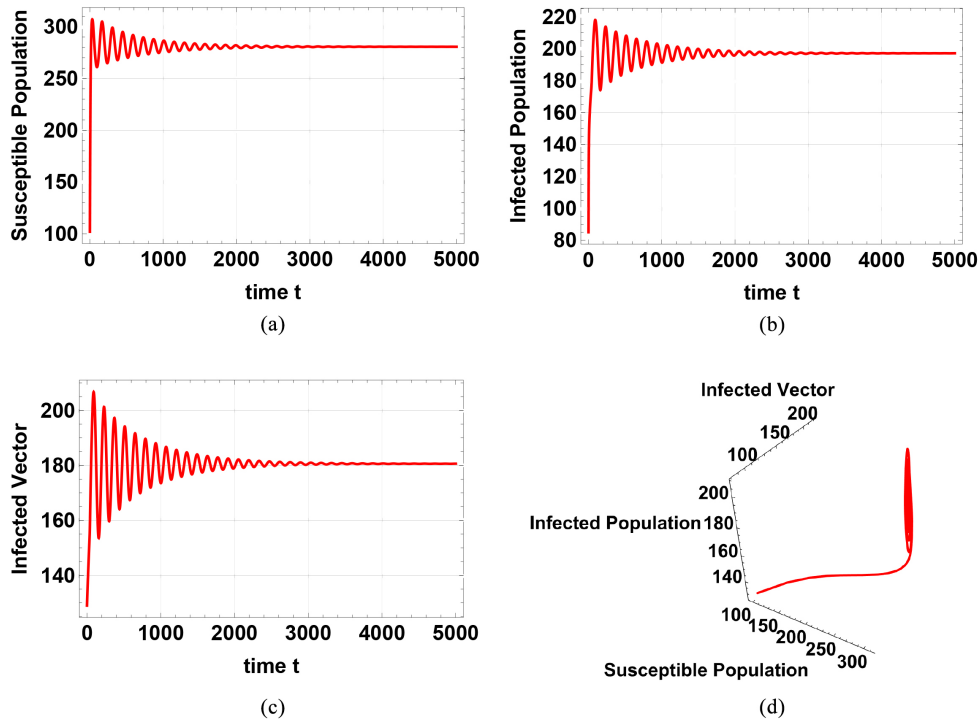


**Fig. 7.** When  $\tau_1 = 0$  and  $\tau_2 = 37 > \tau_2^*$ ,  $E^*$  of the system Eqn. 7 is locally asymptotically stable. (a) The force of the susceptible population converges to the positive equilibrium value  $S_H^* = 280.148$ . (b) The force of the infected population converges to the positive equilibrium value  $I_H^* = 197.053$ . (c) The force of the infected vector converges to the positive equilibrium value  $I_V^* = 180.947$ . (d) Phase diagram of  $E^*$ .

$$d_h) \left( \frac{\Omega_V}{d_v} \right) ] - 2\alpha\beta_v\rho[d_v(\delta + \theta) + \mu_v(\delta + \theta + \rho + d_h)]e^{-d_v\tau_2}$$

$$X_3 = \frac{\alpha^2\beta_h\beta_v(d_v + \mu_v)(\rho e^{-d_h\tau_1} + \sigma d_h) \left( \frac{\Omega_H}{d_h} \right) \left( \frac{\Omega_V}{d_v} \right) e^{-d_v\tau_2} + \alpha^2\beta_h\beta_v\Omega_H \left( \frac{\Omega_V}{d_v} \right) e^{-d_v\tau_2} [e^{-d_h\tau_1}(1 + \mu_v) - \sigma(d_v + \mu_v)] - (\rho + d_h)(\delta + \rho + d_h + \mu_h)(d_v + \mu_v)^2}{2X_1}$$

$$I_1 = \frac{-X_2 + \sqrt{X_2^2 - 4X_1X_3}}{2X_1} \text{ and } I_2 = \frac{-X_2 - \sqrt{X_2^2 - 4X_1X_3}}{2X_1}$$

be the roots of Eqn. 14.

Clearly, we have  $X_1 > 0$ ,  $X_2 > 0$  and  $X_3 > 0$  if  $R_0 < 1$ , and  $X_1 > 0$ ,  $X_3 < 0$  if  $R_0 > 1$ . It is obvious that  $I_1$  and  $I_2$  are negative roots if  $R_0 < 1$ , and that  $I_1$  is positive roots if  $R_0 > 1$ . The following result is drawn from the relationship between the roots Eqn. 14 and the equilibrium of model Eqn. 7.

“If  $R_0 < 1$ , then the system (Eqn. 7) holds illness-free equilibrium  $E^0$ . If  $R_0 > 1$ , then the system (Eqn. 7) holds illness-free equilibrium  $E^0$  and an endemic equilibrium  $E^*$ ”.

#### 4. Stability analysis and Hopf Bifurcation

##### Theorem 2

For  $\tau_1, \tau_2 \geq 0$ , illness-free equilibrium  $E^0$  is locally asymptotically stable if  $R_0 < 1$  and is unstable if  $R_0 > 1$ .

##### Proof

The Jacobian matrix of the system Eqn. 7 at  $E^0$  is

$$J(E_0) = \begin{pmatrix} -d_h - \rho & \theta - \rho & -\alpha\beta_h \frac{\Omega_H}{d_h + \rho} e^{-d_h\tau_1} e^{-\lambda\tau_1} \\ 0 & -(\delta + d_h + \mu_h + \theta) & \alpha\beta_h \frac{\Omega_H}{(d_h + \rho)} [e^{-d_h\tau_1} e^{-\lambda\tau_1} + \frac{\sigma\rho}{d_h}] \\ 0 & \alpha\beta_v \frac{\Omega_V}{d_v} e^{-d_v\tau_2} e^{-\lambda\tau_2} & -(d_v + \mu_v) \end{pmatrix} \quad (15)$$

The characteristic equation of Eqn. 15 is given by

$$(\lambda + d_h + \rho) \{ \lambda^2 + [(\delta + d_h + \mu_h + \theta) + (d_v + \mu_v)] \lambda + (\delta + d_h + \mu_h + \theta)(d_v + \mu_v) [1 - \frac{\alpha^2\beta_h\beta_v\Omega_H\Omega_V e^{-(d_h+\lambda)\tau_1} e^{-(d_v+\lambda)\tau_2}}{(d_h+\rho)d_v(d_v+\mu_v)(\delta+d_h+\mu_h+\theta)} - \frac{\alpha^2\beta_h\beta_v\Omega_H\Omega_V e^{-d_v\tau_2} e^{-\lambda\tau_2} \sigma\rho}{(d_h+\rho)d_v d_h (d_v+\mu_v)(\delta+d_h+\mu_h+\theta)}] \} = 0 \quad (16)$$

One negative eigen value is  $\lambda = -(d_h + \rho)$  and the remaining eigen values of the characteristic equation are

$$\lambda^2 + [(\delta + d_h + \mu_h + \theta) + (d_v + \mu_v)] \lambda + (\delta + d_h + \mu_h + \theta)(d_v + \mu_v) \left[ 1 - R_0 e^{-\lambda(\tau_1 + \tau_2)} \left( 1 + \frac{\sigma\rho}{d_h} e^{d_h\tau_1} e^{\lambda\tau_1} \right) \right] = 0 \quad (17)$$

$$\Rightarrow \lambda^2 + X\lambda + Y = 0$$

$$\text{Where } X = (\delta + d_h + \mu_h + \theta) + (d_v + \mu_v)$$



$$Y = (\delta + d_h + \mu_h + \theta) (d_v + \mu_v) \left[ 1 - R_0 e^{-\lambda(\tau_1 + \tau_2)} \left( 1 + \frac{\sigma \rho}{d_h} e^{d_h \tau_1} e^{\lambda \tau_1} \right) \right]$$

The quadratic equation is the same in the ODE case for  $\tau_1 = \tau_2 = 0$ . In that case, the real component of every eigenvalue of the characteristic equation is already negative. The Hurwitz criterion states that when  $\tau_1 = \tau_2 = 0$ , the illness-free equilibrium  $E^0$  at  $R_0 < 1$  is locally asymptotically stable, however, when  $R_0 > 1$ , it is unstable.

Let us first consider  $R_0 > 1$ . It is simple to demonstrate that Eqn. 17 has a real positive root. Rearranging Eqn. 17 in the form

$$\lambda^2 + X\lambda = (\delta + d_h + \mu_h + \theta)(d_v + \mu_v)[R_0 e^{-\lambda(\tau_1 + \tau_2)}(1 + \frac{\sigma \rho}{d_h} e^{d_h \tau_1} e^{\lambda \tau_1}) - 1] \quad (18)$$

Suppose  $\lambda$  is real. From Eqn. 18, the LHS and RHS are denoted by  $A(\lambda)$  and  $B(\lambda)$  respectively. We have  $A(0) = 0$  and  $\lim_{\lambda \rightarrow \infty} A(\lambda) = \infty$ .

Here,  $B(\lambda)$  is a decreasing function of  $\lambda$

$$B(0) = (\delta + d_h + \mu_h + \theta)(d_v + \mu_v)(R_0 e^{-\lambda(\tau_1 + \tau_2)}(1 + \frac{\sigma \rho}{d_h} e^{d_h \tau_1} e^{\lambda \tau_1}) - 1) > 0$$

As a result, Eqn. 17 has a non-negative real root for any  $\tau_1 \geq 0$  and  $\tau_2 \geq 0$ , and the illness-free equilibrium is destabilizing.

Hence  $E^0$  is locally asymptotically stable in system Eqn. 7 if  $R_0 < 1$  and is unstable if  $R_0 > 1$ .

### Theorem 3

For  $\tau_1 = \tau_2 = 0$ , the endemic equilibrium  $E^*$  is locally asymptotically stable if  $R_0 > 1$  and is unstable if  $R_0 < 1$ .

### Proof

The Jacobian matrix of the system Eqn. 7 of  $E^*$  is

$$J(E^*) = \begin{pmatrix} -d_h - \rho - \alpha\beta_h I_v^* e^{-d_h \tau_1} e^{-\lambda \tau_1} & \theta - \rho & -\alpha\beta_h S_H^* e^{-d_h \tau_1} e^{-\lambda \tau_1} \\ -(\sigma - e^{-d_h \tau_1} e^{-\lambda \tau_1})\alpha\beta_h I_v^* & -\sigma\alpha\beta_h I_v^* - (\delta + d_h + \mu_h + \theta) & \alpha\beta_h S_H^* e^{-d_h \tau_1} e^{-\lambda \tau_1} + \sigma\alpha\beta_h (\frac{\Omega_H}{d_h} - S_H^* - I_H^*) \\ 0 & \alpha\beta_v (\frac{\Omega_V}{d_v} - I_V^*) e^{-d_v \tau_2} e^{-\lambda \tau_2} & -(d_v + \mu_v) - \alpha\beta_v I_H^* e^{-d_v \tau_2} e^{-\lambda \tau_2} \end{pmatrix} \quad (19)$$

The characteristic equation of Eqn. 19 is given by

$$\lambda^3 + k_2 \lambda^2 + k_1 \lambda + k_0 + (l_2 \lambda^2 + l_1 \lambda + l_0) e^{-\lambda \tau_1} + (q_2 \lambda^2 + q_1 \lambda + q_0) e^{-\lambda \tau_2} + (r_1 \lambda + r_0) e^{-\lambda(\tau_1 + \tau_2)} = 0 \quad (20)$$

where

$$\begin{aligned} k_2 &= (\delta + d_h + \mu_h + \theta) + (d_v + \mu_v) + (d_h + \rho) + \sigma\alpha\beta_h I_v^* \\ k_1 &= (\delta + d_h + \mu_h + \theta)(d_v + \mu_v) + \sigma\alpha\beta_h I_v^*(d_v + \mu_v) + (d_h + \rho)[(d_v + \mu_v) + (\delta + d_h + \mu_h + \theta) + \sigma\alpha\beta_h I_v^*] + \sigma\alpha\beta_h I_v^*(\theta - \rho) \\ k_0 &= (d_v + \mu_v)[(d_h + \rho) + (\delta + d_h + \mu_h + \theta) + \sigma\alpha\beta_h I_v^*(d_h + \rho) + \sigma\alpha\beta_h I_v^*(\theta - \rho)] \\ l_2 &= \alpha\beta_h I_v^* e^{-d_h \tau_1} \\ l_1 &= \alpha\beta_h I_v^* e^{-d_h \tau_1} [(\delta + d_h + \mu_h + \theta) + (d_v + \mu_v) + (\rho - \theta) + \sigma\alpha\beta_h I_v^*] \\ l_0 &= \alpha\beta_h I_v^* e^{-d_h \tau_1} [(\delta + d_h + \mu_h + \theta)(d_v + \mu_v) + (\rho - \theta)(d_v + \mu_v) - \sigma\alpha\beta_h I_v^*(d_v + \mu_v)] \\ q_2 &= \alpha\beta_v I_H^* e^{-d_v \tau_2} \\ q_1 &= \sigma\alpha^2 \beta_h \beta_v e^{-d_v \tau_2} I_H^* I_v^* + \sigma\alpha^2 \beta_h \beta_v (\frac{\Omega_H}{d_h} - S_H^* - I_H^*) (\frac{\Omega_V}{d_v} - I_V^*) e^{-d_v \tau_2} + (d_h + \rho)\alpha\beta_v I_H^* e^{-d_v \tau_2} \\ q_0 &= (d_h + \rho)(\delta + d_h + \mu_h + \theta)\alpha\beta_v I_H^* I_v^* e^{-d_v \tau_2} + (d_h + \rho)\sigma\alpha^2 \beta_h \beta_v I_H^* I_v^* e^{-d_v \tau_2} + \sigma\alpha\beta_h (d_h + \rho) (\frac{\Omega_H}{d_h} - S_H^* - I_H^*) \alpha\beta_v (\frac{\Omega_V}{d_v} - I_V^*) e^{-d_v \tau_2} \\ r_1 &= \alpha^2 \beta_h \beta_v I_H^* I_v^* (1 + (\delta + d_h + \mu_h + \theta)) e^{-d_h \tau_1} e^{-d_v \tau_2} - \alpha^2 \beta_h \beta_v S_H^* (\frac{\Omega_V}{d_v} - I_V^*) e^{-d_h \tau_1} e^{-d_v \tau_2} \\ r_0 &= \sigma\alpha^2 \beta_h^2 \beta_v I_v^* I_H^* I_v^* - (\frac{\Omega_H}{d_h} - S_H^* - I_H^*) (\frac{\Omega_V}{d_v} - I_V^*) + S_H^* (\frac{\Omega_V}{d_v} - I_V^*) e^{-d_h \tau_1} e^{-d_v \tau_2} - \alpha^2 \beta_h \beta_v [(d_h + \rho) S_H^* (\frac{\Omega_V}{d_v} - I_V^*) + S_H^* I_v^* (\theta - \rho)] e^{-d_h \tau_1} e^{-d_v \tau_2} \end{aligned}$$

When  $\tau_1 = 0$  and  $\tau_2 = 0$

The characteristic Eqn. 20 becomes

$$\lambda^3 + A_1 \lambda^2 + A_2 \lambda + A_3 = 0 \quad (21)$$

where,  $A_1 = k_2 + l_2 + q_2$ ,  $A_2 = k_1 + l_1 + q_1 + r_1$ ,  $A_3 = k_0 + l_0 + q_0 + r_0$

According to the Routh-Hurwitz criterion, the roots of the characteristic Eqn. 21 does not have a positive real part if and only if the coefficients of  $A_i$  are non negative and matrix  $H_i > 0$ , for  $i = 0, 1, 2, 3$ . From this  $A_1 A_2 - A_3 > 0$ .

Hence the endemic equilibrium  $E^*$  is locally asymptotically stable when  $\tau_1 = \tau_2 = 0$ .

### Theorem 4

For  $\tau_1 > 0$  and  $\tau_2 = 0$ , the endemic equilibrium  $E^*$  is locally asymptotically stable if  $R_0 > 1$  and is unstable if  $R_0 < 1$  [26,27].

### Proof

When  $\tau_1 > 0$  and  $\tau_2 = 0$ , the characteristic Eqn. 20 becomes

$$\lambda^3 + B_1 \lambda^2 + B_2 \lambda + B_3 + (C_1 \lambda^2 + C_2 \lambda + C_3) e^{-\lambda \tau_1} = 0 \quad (22)$$

where  $B_1 = k_2 + q_2$ ,  $B_2 = k_1 + q_1$ ,  $B_3 = k_0 + q_0$ ,  $C_1 = l_2$ ,  $C_2 = l_1 + r_1$  and  $C_3 = l_0 + r_0$

Suppose that  $\lambda = i\omega_0$ ,  $\omega_0 > 0$  then the Eqn. 22 becomes

$$\begin{aligned} B_1 \omega_0^2 - B_3 &= (C_3 - C_1 \omega_0^2) \cos \omega_0 \tau_1 + C_2 \omega_0 \sin \omega_0 \tau_1 \\ \omega_0^3 - B_2 \omega_0 &= - (C_3 - C_1 \omega_0^2) \sin \omega_0 \tau_1 + C_2 \omega_0 \cos \omega_0 \tau_1 \end{aligned} \quad (23)$$

It follows that

$$\begin{aligned} \omega_0^6 + (B_1^2 - 2B_2 - C_1^2) \omega_0^4 + (B_2^2 - C_2^2 - 2B_3 B_1 + 2C_3 C_1) \omega_0^2 + B_3^2 - C_3^2 &= 0 \end{aligned} \quad (24)$$

Denote in  $z = \omega_0^2$  in Eqn. 24

$$g(z) = z^3 + (B_1^2 - 2B_2 - C_1^2)z^2 + (B_2^2 - C_2^2 - 2B_3B_1 + 2C_3C_1)z + (B_3^2 - C_3^2) = 0 \quad (25)$$

$$g(z) = z^3 + h_3z^2 + h_2z + h_1 = 0 \quad (26)$$

where  $h_3 = B_1^2 - 2B_2 - C_1^2$ ,  $h_2 = B_2^2 - C_2^2 - 2B_3B_1 + 2C_3C_1$ ,  $h_1 = B_3^2 - C_3^2$

It is easy to get that  $g'(z) = 3z^2 + 2h_3z + h_2 = 0$  has two roots  $z_1 = \frac{-h_3 + \sqrt{h_3^2 - 3h_2}}{3}$  and  $z_2 = \frac{-h_3 - \sqrt{h_3^2 - 3h_2}}{3}$

Clearly, if  $h_1 \geq 0$ ,  $h_2 \geq 0$  and  $h_3 \geq 0$ , then Eqn. 26 has a negative real root. As a result, Eqn. 22 has negative real parts and has no pure imaginary roots.

Suppose that Eqn. 26 has positive root  $\omega_0$ . A pair of imaginary roots  $(\pm i\omega_0)$ , appear in the characteristic Eqn. 22. Let  $\lambda(\tau_1) = \eta(\tau_1) + i\omega_0(\tau_1)$  be the eigenvalues Eqn. 22 for a certain starting value of the bifurcation parameter  $\tau_1$  then we have  $\eta(\tau_{1k}^n) = 0$ ,  $\omega_0(\tau_{1k}^n) = \omega_0$ .

Denote  $\tau_{1k}^n = \frac{\theta_1 + 2n\pi}{\omega_{0k}}$ ,  $n = 0, 1, 2, \dots$ . Where  $\theta_1 \in [0, 2\pi]$

From Eqn. 23, we get

$$\sin(\theta_1) = \frac{\omega_0^5 C_1 + \omega_0^3 (B_1 C_2 - C_3 - C_1 B_2) + \omega_0 (C_3 B_2 - B_3 C_2)}{(C_3 - C_1 \omega_0^2)^2 + C_2^2 \omega_0^2}$$

$$\cos(\theta_1) = -\frac{\omega_0^4 (B_1 C_1 - C_2) + \omega_0^2 (C_2 B_2 - B_1 C_3 - B_3 C_1) + B_3 C_3}{(C_3 - C_1 \omega_0^2)^2 + C_2^2 \omega_0^2}$$

The following transversality condition also verified.

$$\frac{d}{d\tau_1} \operatorname{Re}(\lambda(\tau)) \Big|_{\tau=\tau_1} = \frac{d}{d\tau_1} \eta(\tau) \Big|_{\tau=\tau_1} > 0 \text{ holds.}$$

By continuity, when  $\tau_1 > \tau_1^*$  and the real part of  $\lambda(\tau_1)$  turns positive, the steady state is unstable. Furthermore, the Hopf bifurcation occurs when  $\tau_1$  reaches the crucial value in  $\tau_1^*$  [23]. When  $\tau_2 = 0$ ,  $\tau_1 > \tau_2$ , the equilibrium  $E^*$  is asymptotically stable. However, if  $\tau_1^*$  remains in a certain right neighbourhood of  $\tau_1$ , the equilibrium  $E^*$  becomes unstable.

Hence, the Hopf bifurcation occurs when  $\tau_1^* = \tau_1$ .

### Theorem 5

For  $\tau_1 = 0$  and  $\tau_2 > 0$ , the endemic equilibrium  $E^*$  is locally asymptotically stable if  $R_0 > 1$  and is unstable if  $R_0 < 1$ . Hopf bifurcation occurs when  $\tau_2 = \tau_2^*$ , at the equilibrium  $E^*$  of the system Eqn. 7.

### Proof

When  $\tau_1 = 0$  and  $\tau_2 > 0$ , the characteristic Eqn. 20 becomes

$$\lambda^3 + D_1 \lambda^2 + D_2 \lambda + D_3 + (E_1 \lambda^2 + E_2 \lambda + E_3) e^{-\lambda \tau_2} = 0 \quad (27)$$

where  $D_1 = k_2 + l_2$ ,  $D_2 = k_1 + l_1$ ,  $D_3 = k_0 + l_0$ ,  $E_1 = q_2$ ,  $E_2 = q_1 + r_1$  and  $E_3 = q_0 + r_0$

Suppose that  $\lambda = i\omega_1$ ,  $\omega_1 > 0$  then the Eqn. 27 be-

comes

$$D_1 \omega_1^2 - D_3 = (E_3 - E_1 \omega_1^2) \cos \omega_1 \tau_2 + E_2 \omega_1 \sin \omega_1 \tau_2$$

$$\omega_1^3 - D_2 \omega_1 = -(E_3 - E_1 \omega_1^2) \sin \omega_1 \tau_2 + E_2 \omega_1 \cos \omega_1 \tau_2 \quad (28)$$

It follows that

$$\omega_1^6 + (D_1^2 - 2D_2 - E_1^2) \omega_1^4 + (D_2^2 - E_2^2 - 2D_3 D_1 + 2E_3 E_1) \omega_1^2 + D_3^2 - E_3^2 = 0 \quad (29)$$

Denote  $z = \omega_1^2$  in Eqn. 29

$$f(z) = z^3 + (D_1^2 - 2D_2 - E_1^2) z^2 + (D_2^2 - E_2^2 - 2D_3 D_1 + 2E_3 E_1) z + (D_3^2 - E_3^2) = 0 \quad (30)$$

Let  $j_3 = D_1^2 - 2D_2 - E_1^2$ ,  $j_2 = D_2^2 - E_2^2 - 2D_3 D_1 + 2E_3 E_1$ ,  $j_1 = (D_3^2 - E_3^2)$  then Eqn. 30 is

$$f(z) = z^3 + j_3 z^2 + j_2 z + j_1 = 0 \quad (31)$$

It is easy to get that  $f'(z) = 3z^2 + 2j_3 z + j_2 = 0$  has two roots  $z_1 = \frac{-j_3 + \sqrt{j_3^2 - 3j_2}}{3}$  and  $z_2 = \frac{-j_3 - \sqrt{j_3^2 - 3j_2}}{3}$

Clearly, if  $j_1 \geq 0$ ,  $j_2 \geq 0$  and  $j_3 \geq 0$ , then Eqn. 31 has negative real roots. Hence, Eqn. 27 has negative real parts and does not have any pure imaginary roots.

If we assume that Eqn. 31,  $z_1$ ,  $z_2$  and  $z_3$  are three positive roots, then  $\omega_1 = \sqrt{z_1}$ ,  $\omega_2 = \sqrt{z_2}$  and  $\omega_3 = \sqrt{z_3}$  are three positive numbers.

From Eqn. 28

$$\cos \omega_1 \tau_2 = \frac{(D_1 \omega_1^2 - D_3)(E_3 - E_1 \omega_1^2) + E_2 \omega_1 (\omega_1^3 - D_2 \omega_1)}{(E_3 - E_1 \omega_1^2)^2 + E_2^2 \omega_1^2}$$

Denote

$$\tau_{2k}^n = \frac{1}{\omega_{1k}} \arccos \left\{ \frac{(D_1 \omega_1^2 - D_3)(E_3 - E_1 \omega_1^2) + E_2 \omega_1 (\omega_1^3 - D_2 \omega_1)}{(E_3 - E_1 \omega_1^2)^2 + E_2^2 \omega_1^2} \right\} +$$

$\frac{2n\pi}{\omega_{1k}}$

and  $\tau_2^* = \min_{1 \leq k \leq m} \tau_{2k}^{(0)}$ ,  $\omega_1 = \omega_i$ ,  $i = 1, 2, 3, \dots, m$

where  $\omega_1$  is corresponds to  $\tau_2^*$ .

Let  $\lambda(\tau_2) = \eta(\tau_2) + i\omega_1(\tau_2)$  be the eigenvalues of the characteristic Eqn. 27 satisfying  $\eta(\tau_{2k}^n) = 0$ ,  $\omega_1(\tau_{2k}^n) = \omega_1$ .

From Eqn. 27, we get  $(\frac{d\lambda}{d\tau_2})^{-1} = \frac{P_1 + iP_2}{P_3 + iP_4}$

where,

$$P_1 = (E_3 - E_1 \omega_1^2)[(-3\omega_1^2 + D_2) + \tau_2(-D_1 \omega_1^2 + D_3)] + (D_2 \omega_1 - \omega_1) \omega_1 (2E_1 - \tau_2 E_2) - E_2 [2D_1 \omega_1^2 + (-D_1 \omega_1^2 + D_3)]$$

$$P_2 = (E_3 - E_1 \omega_1^2) [2D_1 \omega_1 + \tau_2 (D_2 \omega_1 - \omega_1)] + \omega_1 (-\omega_1^2 D_1 + D_3) (\tau_2 E_2 - 2E_1) + E_2 [\omega_1 (-3\omega_1^2 + D_2) - (D_2 \omega_1 - \omega_1)]$$

$$P_3 = E_2 \omega_1^2 (-\omega_1^2 D_1 + D_3) + (E_3 \omega_1 - E_1 \omega_1^3) (D_2 \omega_1 - \omega_1)$$

$$P_4 = (E_1 \omega_1^3 - E_3 \omega_1) (-\omega_1^2 D_1 + D_3) - E_3 \omega_1 (-\omega_1^2 D_1 + D_3) + E_2 \omega_1^2 (D_2 \omega_1 - \omega_1)$$

Therefore,  $\operatorname{Re}(\frac{d\lambda}{d\tau_2})^{-1} \Big|_{\lambda=i\omega_0} = \frac{P_1 P_3 + P_2 P_4}{P_3^2 + P_4^2}$

If  $P_1 P_3 + P_2 P_4 \neq 0$  then  $\operatorname{Re}(\frac{d\lambda}{d\tau_2})^{-1} \Big|_{\lambda=i\omega_0} \neq 0$  hold.

If  $\tau_1 = 0$  and  $P_1 P_3 + P_2 P_4 \neq 0$  the  $E^*$  is asymptotically stable when  $\tau_2 \in [0, \tau_2^*)$ .

Hence, the Hopf bifurcation occurs when  $\tau_2^* = \tau_2$ .

## 5. Numerical Simulations

Theorems 2, 3, 4, and 5 explore the stability of an endemic equilibrium, which is important from an epidemiological perspective. The parameter values of the model is showed in Table 2 (Ref. [3,21]).

**Table 2. Parameter and values of the model.**

Parameter	Value	Source
$\Omega_H$	9	Yanxia <i>et al.</i> [21]
$\Omega_V$	10	Yanxia <i>et al.</i> [21]
$\beta_h$	0.002	Yanxia <i>et al.</i> [21]
$\beta_v$	0.005	Yanxia <i>et al.</i> [21]
$d_h$	0.01	Yanxia <i>et al.</i> [21]
$d_v$	0.05	Yanxia <i>et al.</i> [21]
$\mu_h$	0.05	Hui, Jing-An [3]
$\mu_v$	0.1	Hui, Jing-An [3]
$\alpha$	0.3	Yanxia <i>et al.</i> [21]
$\theta$	0.08	Hui, Jing-An [3]
$\delta$	0.2	Assumed
$\sigma$	0.8	Yanxia <i>et al.</i> [21]
$\rho$	0.02	Assumed

By Theorem 3, when  $\tau_1 = \tau_2 = 0$  the stability of the endemic equilibrium  $E^*$  (267.781, 210.142, 196.792) is converging towards being locally asymptotically stable (Fig. 2). It is tougher to control the disease as  $R_0 = 3.17647 > 1$  and dengue fever persists in both human and vector populations.

When  $\tau_1 > 0, \tau_2 > 0$ , the stability of the endemic equilibrium  $E^*$  (339.886, 180.022, 183.872) is converging towards locally asymptotically stable (Fig. 3). As  $R_0 = 0.499459 < 1$  is obtained, dengue fever disappears in both the human and vector populations, making it simpler to stop the disease's spread.

By Theorem 4, if  $\tau_1 = 32.8$  and  $\tau_2 = 0$ , the stability of the endemic equilibrium  $E^*$  (333.986, 188.115, 196.753) is converging towards being locally asymptotically stable (Fig. 4). Dengue fever is more difficult to control as  $R_0 = 2.28821 > 1$  and the human and vector populations remain infected. If  $\tau_1 > 32.8$  and  $\tau_2 = 0$ , the stability of the endemic equilibrium  $E^*$  is diverging towards instability and its  $E^*$  loses stability as  $\tau_1$  passes through  $\tau_1^*(32.9)$ , leading to a Hopf bifurcation (Fig. 5).

By Theorem 5, if  $\tau_1 = 0$  and  $\tau_2 < 36.9$ , the stability of the endemic equilibrium  $E^*$  is diverging towards instability, resulting in a bifurcation when  $\tau_2$  passes upon  $\tau_2^*(36.8)$  (Fig. 6). If  $\tau_1 = 0$  and  $\tau_2 = 37$ , the stability of the endemic equilibrium  $E^*$  (280.148, 197.053, 180.947) is converging towards being locally asymptotically stable (Fig. 7). As  $R_0 = 0.499459 < 1$  is obtained, dengue fever disappears in both human and vector populations, making it simpler to stop the disease's spread.

In every instance, the stability of the endemic equilibrium  $E^*$  is comparatively higher than that of the existing

literature [21], which strengthens the model we have created.

## 6. Conclusions

In this study, positivity and boundedness were verified for the solution of the dengue transmission dynamic model. The basic reproduction number  $R_0$  was chosen to ensure the model's stability. It was established that the two delayed models' endemic equilibrium  $E^*$  and illness-free equilibrium  $E^0$  both existed. The steadiness of illness-free equilibrium was determined for  $\tau_1, \tau_2 \geq 0$  in terms of  $R_0$ . The steadiness of endemic equilibrium was determined for  $\tau_1 = \tau_2 = 0; \tau_1 > 0$  and  $\tau_2 = 0; \tau_1 = 0$  and  $\tau_2 > 0$  in terms of positivity of  $R_0$ . The local asymptotic stability of the endemic equilibrium  $E^*$  occurs when  $\tau_1 = \tau_2 = 0$ . The endemic equilibrium becomes unstable and undergoes Hopf bifurcation if  $\tau_2 = 0$  and  $\tau_1 > \tau_1^*$ . Similarly, the endemic equilibrium becomes unstable and undergoes Hopf bifurcation if  $\tau_1 = 0$  and  $\tau_2 < \tau_2^*$ . As a result, the endemic equilibrium is locally asymptotically stable if two delays are greater than zero. Our numerical simulations clearly demonstrate that, whereas susceptible and infected population levels are initially unstable, they become stable as time moves on. The length of the delay has no effect on the stability of the illness-free equilibrium. The Hopf bifurcation might occur nonetheless, depending on how much the delay affects the underlying equilibrium's stability. Future research will expand on this assessment to examine the effects of a few control measures built into our model. The best way to control the disease will be examined as well, taking into account a variety of prevention strategies like self-defense, medical attention, and insecticide spraying.

### Medical Implication of Mathematical Study

In this paper, mosquito-borne dengue fever viruses (DENV) were studied with the help of two delays. We have observed the following medical implications as mathematical observations.

Since the basic reproduction number is given by  $R_0$ , if  $R_0 < 1$ , the disease does not survive, and if  $R_0 > 1$ , the disease keeps spreading, the infection rate will increase. The results are mostly favorable to  $R_0 > 1$ , but it requires good medical treatment, and the patients are also required to have the place very clean, free from stagnant water and unwanted materials around the shelter, to reduce the reproduction of dengue-spreading mosquitoes. Bifurcation in mathematical theory is used to verify the topological structure of the solutions of the system of differential equations. This is not a quantitative result, but it provides a qualitative assessment of whether the system is stable or not after some transition time. Medically, the bifurcations can be understood as a visualization of the possibility of a group of infective hosts becoming healthy or not. By our numerical simulations, we can easily see that initially the populations of susceptibles and infected were not stable, but as time increased, they be-

came stable. It clearly shows that, medically, it is possible to bring society back to being free from dengue.

Other than the basic reproduction number, stability analysis, and bifurcation analysis, we also like to mention a few points shared by the World Health Organization (WHO) [28]. DENV is caused by females of the mosquito species *Aedes aegypti* and rarely by *Albopictus*.

Severe dengue is a very deadly disease, as it causes serious illness and death in some Asian and Latin American countries. It requires management by medical experts. Though Dengue has various epidemiological structures (DENV-1, DENV-2, DENV-3 and DENV-4) produced by the Flaviviridae family of viruses, there is a strong belief that once recovered from this disease, one will have a lifelong immunity against the same [29].

As we have mentioned, medically, there is no proper treatment for the later stages of dengue. Therefore, mathematical modeling is useful to provide qualitative analyses for the chance of recovery for a large infected community.

### Availability of Data and Materials

All the datasets and materials from which the entire study was done are available within the manuscript.

### Author Contributions

Conceptualization – PRM, VA, VS; Supervision – VA, VS, DB; Writing – original draft – PRM, PBD, DB; Numerical results – PRM, VS, PBD; Analysis & Verification – PRM, VA, DB; Final draft-proof reading – PRM, VA, VS, PBD, DB. All authors contributed to editorial changes in the manuscript. All authors read and approved the final manuscript. All authors read and approved the final manuscript. All authors have participated sufficiently in the work and agreed to be accountable for all aspects of the work.

### Ethics Approval and Consent to Participate

Not applicable.

### Acknowledgment

Not applicable.

### Funding

This research received no external funding.

### Conflict of Interest

The authors declare no conflict of interest. DB is serving as one of the Guest editors of this Journal. We declare that DB had no involvement in the peer review of this article and has no access to information regarding its peer review. Full responsibility for the editorial process for this article was delegated to GP.

## References

- [1] Pragati D and Irrusappan H. Vector-Borne Diseases in India. *International Journal of Advanced Research*. 2020; 8: 1055–1067.
- [2] Hu Z, Yin S, Wang H. Stability and Hopf Bifurcation of a Vector-Borne Disease Model with Saturated Infection Rate and Reinfection. *Computational and Mathematical Methods in Medicine*. 2019; 2019: 1352698.
- [3] Hui W and Jing-An C. A Model for the transmission of Malaria. *Discrete and Continuous Dynamical Systems Series B*. 2009; 11: 479–496.
- [4] Khan MA, Iqbal N, Khan Y, Alzahrani E. A biological mathematical model of vector-host disease with saturated treatment function and optimal control strategies. *Mathematical Biosciences and Engineering: MBE*. 2020; 17: 3972–3997.
- [5] Alshorman A, Wang X, Joseph Meyer M, Rong L. Analysis of HIV models with two time delays. *Journal of Biological Dynamics*. 2017; 11: 40–64.
- [6] Vinoth S, Jayakumar T, Prasantha Bharathi D. Analysis of a delayed HIV pathogenesis model with saturation incidence, both virus-to-cell and cell-to-cell transmission. *International Journal of Nonlinear Analysis and Applications*. 2022; 13: 1927–1936.
- [7] Xin J. Threshold dynamics of a general delayed HIV model with double transmission models and latent viral infection. *AIMS Mathematics*. 2021; 7: 2456–2478.
- [8] Ruan S, Xiao D, Beier JC. On the delayed Ross-Macdonald model for malaria transmission. *Bulletin of Mathematical Biology*. 2008; 70: 1098–1114.
- [9] Muthu P, Bikash M. Study of a Delayed SIVA Within-Host Model of Dengue Virus Transmission. *Communication in Biomathematical Sciences*. 2022; 5: 101–120.
- [10] Sefidgar E, Celik E, Shiri B. Numerical Solution of Fractional Differential Equation in a Model of HIV Infection of CD4+T Cells. *International Journal of Applied Mathematics and Statistics*. 2017; 56: 23–32.
- [11] Wei HM, Li XZ, Martcheva M. An epidemic model of a vector-borne disease with direct transmission and time delay. *Journal of Mathematical Analysis and Applications*. 2008; 342: 895–908.
- [12] Omame A, Abbas M, Abdel-Aty AH. Assessing the impact of SARS-CoV-2 infection on the dynamics of dengue and HIV via fractional derivatives. *Chaos, Solitons, and Fractals*. 2022; 162: 112427.
- [13] Omame A, Rwezaura H, Diagne ML, Inyama SC, Tchuenche JM. COVID-19 and dengue co-infection in Brazil: optimal control and cost-effectiveness analysis. *European Physical Journal Plus*. 2021; 136: 1090.
- [14] Wan H, Cui J. A malaria model with two delays. *Discrete Dynamics in Nature and Society*. 2013; 10: 8
- [15] Xu J, Zhou Y. Hopf Bifurcation and its stability for a vector-borne disease model with delay and Reinfection. *Applied Mathematical Modelling*. 2016; 40: 1685–1702.
- [16] Zizhen Z, Soumen K, Jai Prakash T, Sarita B. Stability and Hopf bifurcation analysis of an SVEIR epidemic model with vaccination and multiple time delays. *Chaos, Solitons and Fractals*. 2020; 131: 17.
- [17] Dumitru B, Babak S. Generalized fractional differential equations for past Dynamic. *International journal of applied mathematics and statistics*. *AIMS Mathematics*. 2022; 7: 14394–14418
- [18] Kalpana U, Balaganesan P, Renuka J, Dumitru B, Prasantha Bharathi D. On the decomposition and analysis of novel simultaneous SEIQR epidemic model. *AIMS Mathematics*. 2023; 8: 5918–5933.
- [19] Rangasamy M, Chesneau C, Martin-Barreiro C, Leiva V. On a novel dynamic of SEIR epidemic models with a potential application to COVID-19. *Symmetry*. 2022; 14: 1436.

- [20] Rangasamy M, Alessa N, Dhandapani PB, Loganathan K. Dynamics of a novel IVRD pandemic model of a large population over a long time with efficient numerical methods. *Symmetry*. 2022; 14: 1919.
- [21] Yanxia Z, Long L, Junjian H, Yanjun L. Stability and Hopf Bifurcation Analysis of a Vector-Borne Disease Model with Two Delays and Reinfection. *Computational and Mathematical Methods in Medicine*. 2021; 18: 17.
- [22] Wu C, Wong PJY. Dengue transmission: mathematical model with discrete time delays and estimation of the reproduction number. *Journal of Biological Dynamics*. 2019; 13: 1–25.
- [23] Hale J. *London Mathematical Society Lecture Note series: Theory and application of Hopf bifurcation*. Cambridge University Press: Cambridge, UK. 1977.
- [24] Hassard BD, Kazarinoff ND, Wan YH. *London Mathematical Society Lecture Note series 41: Theory and application of Hopf bifurcation*, Cambridge University Press: Cambridge, UK. 1981.
- [25] Diekmann O, Heesterbeek JA, Metz JA. On the definition and the computation of the basic reproduction ratio  $R_0$  in models for infectious diseases in heterogeneous populations. *Journal of Mathematical Biology*. 1990; 28: 365–382.
- [26] Vinoth S, Jayakumar T, Prasantha Bharathi D. Dynamics of Two Delays Differential Equations Model of HIV Pathogenesis with Absorption and saturation Incidence. *Discontinuity, Nonlinearity, and Complexity*. 2021; 10: 435–444.
- [27] Vinoth S, Dumitru B, Jayakumar T, Prasantha Bharathi D. Analysis of time delay model for drug therapy on HIV dynamics. *Computational Methods for Differential Equations*. 2021; 9: 577–588.
- [28] World Health Organization. 2023. Available at: <https://www.who.int/news-room/fact-sheets/detail/dengue-and-severe-dengue> (Accessed: 17 March 2023).
- [29] Srinivas V, and Srinivas VR. Dengue fever: A review article. *Journal of Evolution of Medical and Dental Sciences*. 2011; 4: 5048–5058.